Density Relaxation of Liquid-Vapor Critical Fluids in Earth's Gravity

R. Allen Wilkinson*

^{*}Microgravity Fluid Physics Branch, NASA Lewis Research Center, Cleveland, OH 44135, USA.

Abstract

Experimental results of the density relaxation of a liquid-vapor critical fluid in earth's gravity over a temperature regime of severe density stratification are presented. A dime-shaped sample of SF₆ was placed in a Twyman-Green phase shifting interferometer with a phase uncertainty of $\lambda/65$ over 60 hours. Relaxations to equilibrium stratification were observed for a temperature range from $T_c+1.0$ mK to $T_c+29.6$ mK, where T_c is the critical temperature. The interferometry provided density data as a continuous function of height and time over the full extent of the sample cell.

Two types of initial density states were established before stepping to the final temperature (density) states for relaxation; 1) the two phase state at $T_c - 50$ mK, and 2) the equilibrium state at $T_c + 100$ mK. Upper and lower portions of the cell relaxed differently for these two initial states. For the $T_c + 100$ mK initial state, relaxation to $T < T_c + 3$ mK showed a density overshoot followed by an additional long-time relaxation not seen in the other relaxation sequences. Otherwise, relaxations were faster and non-diffusive as the final state became closer to the critical temperature.

Key Words: critical point, equilibration, liquid-vapor critical point, sulfur hexafluoride, compressible fluid, thermal equilibrium.

1 INTRODUCTION

Typically, Earth-based room temperature liquid-vapor critical fluid experiments have not been performed closer than 30 mK above the critical temperature, T_c , because of gravitational stratification effects[1]. However, there are some early theory and experiments that considered thermal relaxation times and mechanisms in this regime[2, 3, 4, 5]. From the 1980's to the present there have been a number of microgravity experiments that examined equilibration[6] and have been performed with $\varepsilon < 10^{-4}$, $\varepsilon \equiv \frac{T-T_c}{T_c}[7, 8, 9, 10]$. Those experiments resolved some early confusion about how fast a critical fluid equilibrates in low gravity. To complement the low gravity experiments, this paper presents similar experiments in Earth's gravity.

In recent years several groups have worked on experiments and models [11, 12, 13, 14] to describe density relaxation of one-phase systems in Earth's gravity. The models have examined one or two dimensions, considered small or slow temperature changes relatively far from T_c , and used fixed thermophysical properties to allow linearization in the models. Other groups have worked on the equilibration of critical binary mixtures as they transition from a two-phase state to a one-phase state by tracking the surface tension evolution [15, 16]. The complete understanding of liquid-vapor critical fluid equilibration in 1-g is more difficult than in low-g, because divergent thermophysical properties and compressible fluid hydrodynamics mix in complicated ways.

The observation of choice in this work was interferometric imaging. The technique allowed resolution in two dimensions with no thermal or geometrical pertubation to the sample.

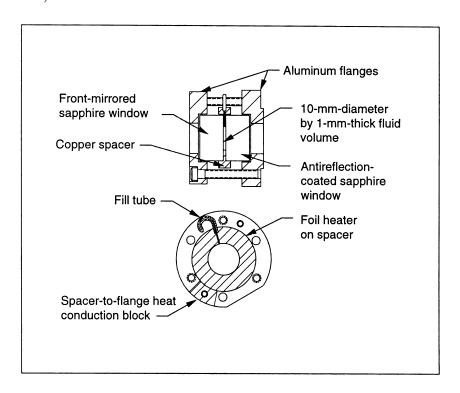
This paper presents experimental observations with two kinds of intial conditions and relatively large temperature changes to the final state. Section 2 will present some of the experimental configuration and procedures. Section 3 will present results, and section 4 will offer conclusions.

2 EXPERIMENTAL

This work collected Earth-based interferometric data from a 10 mm diameter by 1 mm thick disk volume of sulfur-hexafluoride (an equivalent sample to that used for low-g experiments[10]). The gravity-vector is along a diameter of the disk. The interferometer was a compact Twyman-Green configuration contained inside a thermostat with better than $\pm 50~\mu\text{K}$ control. The cell is loaded to $\rho_c - 0.05\%(+0.20\text{-}0.00\%)$, where ρ_c is the critical density. The density precision was determined by measuring the meniscus location just below T_c with respect to the location of a model perfectly filled cell. The critical temperature was $45.4630~\pm 0.0003~\text{C}$ as measured repeatedly with a thermistor calibrated by the manufacturer to $\pm 0.1~\text{C}$. The uncertainty in T_c is primarily caused by ambiguity of the appearance of the phase transition in a stratified sample viewed interferometrically.

The thermostat consisted in-part of two PID-controlled temperature shells of aluminum. A third, the inner-most, shell was a 11 cm long by 6 cm diameter aluminum sample cell holder. The sample cell holder contained the fluid cell and the Twyman-

Figure 1: Fluid cell for interferometric measurements. The foil heater was not used in this work. (Ed. note: This figure looks best on-screen when magnified 300% or more. It prints fine.)



Green interferometer. The compact interferometer under tight temperature control greatly enhanced optical phase resolution. The short-term phase resolution in this work was better than $\lambda/470$, while the long-term phase resolution was $\lambda/65$ over 60 hours. The cell, shown schematically in Fig. 1, was designed for minimal thermal gradients and low thermal mass. Temperature changes from the initial to the final temperature state required 15 to 19 minutes, with no overshoot. The optical layout details are best described in the complementary paper on phase shifting interferometry[17].

Experimental operations were automated for both temperature control and image capture with runs up to 50 hours in duration. Image capture sequences were executed 16 times in less than six seconds to constitute one snapshot of the fluid density.

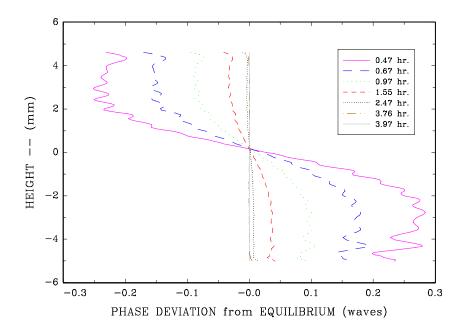
A data set consisted of four final states (nominally 30 mK, 10 mK, 3 mK, and 1 mK above T_c) from each of two initial states (100 mK above T_c and 50 mK below T_c). Hence, there were eight runs in a data set. A run would last more than five time-constants as predicted from a diffusive model and low-gravity experiments. There were at least 100 capture sequences during a run.

The phase shifting Twyman-Green interferometer was set up to use the Carré technique of analysis. The technique required four images per optical phase map. Four sets of four images were captured to provide some statistical averaging. The Carré technique produced a two-dimensional pixel-wise array of phase values for each snapshot in time. An array was 540 pixels high by 480 pixels wide in each image and phase map. The last phase map in a run was used as a reference map and subtracted from all the other maps. This eliminated fixed phase shifts in the optics and referenced the data with respect to a nominal fluid equilibrium. Pixels beyond the fluid boundary were masked out in the final analysis.

The 540 horizontal layers were divided into groups of three and assigned a height with respect to the horizontal layer where the meniscus forms. There were 168 such grouped layers that spanned the 1 cm fluid diameter. All the pixels in each of the layer groups were averaged to determine a phase shift per height. Each average included 700 to 1400 pixels. A data set then provides a measure of fluid density deviation from

equilibrium as a function of height and time, Fig. 2.

Figure 2: Height profiles of deviation from equilibrium in time for a run with the initial state of $T_c - 50$ mK and a final state of $T_c + 29.6$ mK. The earliest and latest times plotted reflect the time window when the thermostat was stable to $\pm 50 \ \mu \text{K}$.



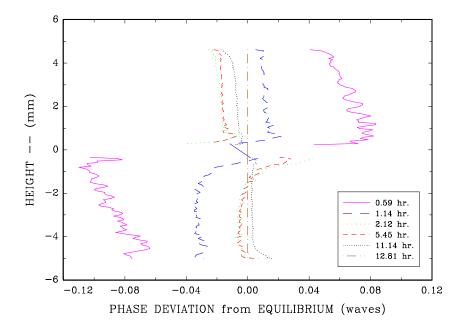
The final step of analysis was the fitting of a time sequence of deviations at a given height to an exponetial function that was used for the low-gravity experiments[10]. The fitting function was

$$K + A \left\{ e^{(-t/\tau)} - e^{(-t_r/\tau)} \right\},$$
 (1)

where t is time, t_r is the time of the reference phase map that is subtracted, and K, A, and τ are fitting parameters.

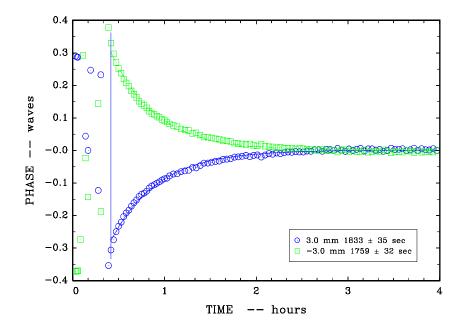
3 RESULTS

Compare Figures 2 and 3 to see extreme examples of the fluid's behavior. Note, four Figure 3: Height profiles for a run with the initial state of $T_c + 100$ mK and a final state of $T_c + 2.8$ mK. Note the geometric time sequence of the plots. Ignore the traces ± 0.5 mm about 0.0 because the fringes were too closely packed for reliable analysis.



waves of phase shift are about 1.4% fluid density deviation. In those figures one sees different behavior between the upper and lower cell halves, and a conspicuous density overshoot in each half of the cell in Fig. 3. There is a visible ripple in the traces of both figures that diminishes with time. The ripple evident in the one-phase to one-phase relaxation contains more spatial frequencies than in the two-phase to one-phase relaxation. This ripple is evident even when the thermometry is stable to

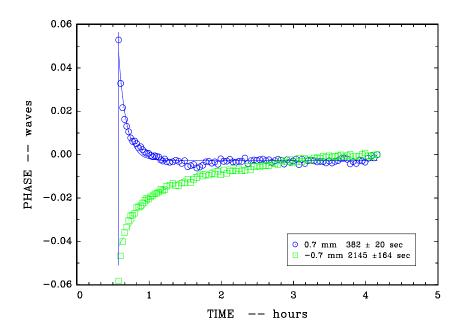
Figure 4: Relaxation at 3 mm above and below the meniscus for a run with an initial state at $T_c - 50$ mK and a final state of $T_c + 29.6$ mK. In low-gravity the time constant was 1087 ± 10 seconds at $T_c + 28.7$ mK. The vertical line early in the plot was marked the beginning of the fit to Eqn.1.



our specification. The initial temperature change transients of a run provided a severe perturbation of the fluid this close to the critical point. The interpretation of the ripple observation is that the fluid boundary layers on the sapphire windows are not of uniform thickness and changing with time. One might expect flows of different character in these two runs.

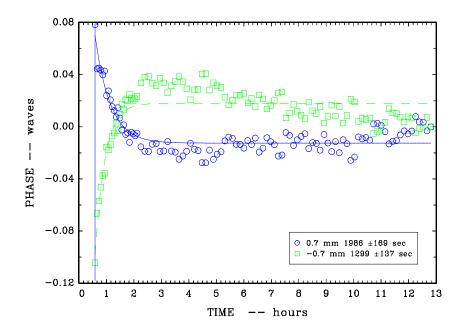
Consider next the time dependence at selected heights. Figure 4 represents the best fit to Eqn.1. For this run the time constant was significantly longer at all heights in the sample than it was for the low-g experiment. The run begins to overlap with the

Figure 5: Relaxation at 0.7 mm above and below the meniscus for a run with an initial state at $T_c + 100$ mK and a final state of $T_c + 29.6$ mK.



temperature regime being explored by Maher[15]. Figure 5 represents a run where the initial state, $T_c + 100$ mK, was different than in fig. 4. The height position was selected closer to the meniscus to show best the beginning asymmetry of the relaxation in the vapor-like and liquid-like portions of the cell. In low-gravity, relaxation results were not sensitive to the initial state being two-phase or one-phase[10]. Figure 6 represents further anomalies for a one-phase to one-phase experiment run. With the final state at $T_c + 2.8$ mK one sees two quite different relaxation time scales. It appears that the longest time scale is not completely captured even in the more than eight time constants predicted from low-gravity work. An overshooting of the density occurs in both the liquid-like and vapor-like portions of the fluid, still with an asymmetry.

Figure 6: Relaxation at 0.7 mm above and below the meniscus for a run with an initial state at $T_c + 100$ mK and a final state of $T_c + 2.8$ mK. In low-gravity the time constant was 5546 ± 62 seconds at $T_c + 3.4$ mK.



4 CONCLUSIONS

From this sequence we see that an exponential decay becomes a poorer and poorer fit the closer to Tc and the closer to the critical region near the meniscus one gets. We also see that relaxing from an initial one-phase state (e.g. $T_c + 100 \,\mathrm{mK}$) produces a worse fit to exponential decay than relaxing from a two-phase state. In fact, a one-phase initial state gives rise to an overshoot of the density during the early relaxation to $T < T_c + 5 \,\mathrm{mK}$ followed by a very long relaxation that we have not yet waited enough to capture. Two-phase to one-phase relaxations were faster than diffusion close to T_c ,

but suggest that for $T \geq T_c + 30\,\mathrm{mK}$ relaxations become slower than diffusive.

5 ACKNOWLEDGEMENTS

This work was performed at NASA Lewis Research Center in Cleveland, Ohio as part of the Microgravity Fluid Physics Branch. The author would like to thank Christoph Bartscher, Mike Bayda, and Gary Fiedler for substantial help in setting up the experiment. Also the understanding of this work has benefitted greatly from discussions with Hacene Boukari, Robert Berg, Robert Gammon, Greg Zimmerli, Kyung-Yang Min, James Maher, and Horst Meyer.

References

- M. R. Moldover, J. V. Sengers, R. W. Gammon, and R. J. Hocken, Rev. Mod. Phys., 51:79 (1979).
- [2] M. Sh. Giterman and V. A. Shteinberg, Teplofizika Vyslokikh Temperatur, 10:565(1972). [High Temp., 10:501 (1972)].
- [3] D. Dahl and M. R. Moldover, Phys. Rev. A, **6:**1915 (1972).
- [4] M. Gitterman, Rev. Mod. Phys., **50**:85, Part I (1978).
- [5] T. J. Edwards, "Specific Heat Measurements Near the Critical Point of Carbon Dioxide", Ph.D. thesis, Department of Physics, Univ. of Western Australia (1984).

- [6] H. Klein and B. Feuerbacher, Phys. Lett. A, 123:183 (1987).
- [7] J. Straub and K. Nitsche, Fluid Phase Equil., 88:183 (1993).
- [8] J. Straub, L. Eicher, and A. Haupt, Phys. Rev. E, **51**:5556 (1995).
- [9] T. Fröhlich, P. Guenoun, M. Bonetti, F. Perrot, D. Beysens, Y. Garrabos, B. LeNeindre, and P. Bravais, Phys. Rev. E, 54:1544 (1996).
- [10] R. A. Wilkinson, G. A. Zimmerli, H. Hao, M. R. Moldover, R. F. Berg, W. L. Johnson, R. A. Ferrell, and R. W. Gammon, Phys. Rev. E, (submitted 1997).
- [11] R. F. Berg, Phys. Rev. E, 48, 1799 (1993).
- [12] H. Boukari, R. L. Pego, and R. W. Gammon, Phys. Rev. E, 52, 1614 (1995).
- [13] F. Zhong and H. Meyer, Phys. Rev. E, **51**, 322 (1995).
- [14] B. Zappoli, S. Amiroudine, P. Carles, and J. Ouazzani, J. Fluid Mech., 316, 53 (1996).
- [15] S. E. May and J. V. Maher, Phys. Rev. Lett., **67**:2013 (1991).
- [16] W-J. Ma, P. Keblinski, A. Maritan, J. Koplik, J. R. Banavar, Phys. Rev. Lett., 71:3465 (1993).
- [17] M. R. Bayda, C. Bartscher, R. A. Wilkinson, and G.A. Zimmerli, "High Resolution Phase Shifting Interferometer", Proc. Thirteenth Symposium on Thermophysical Properties, NIST, Boulder, CO, US (1997).